The International Journal of Advanced Manufacturing Technology (2019) 101:1583–1593
https://doi.org/10.1007/s00170-018-3013-7

ORIGINAL ARTICLE

An investigation in the ultra-precision fly cutting of freeform surfaces on brittle materials with high machining efficiency and low tool wear

Zhanwen Sun [1] · Suet To [1] · K. M. Yu [1]

Received: 30 August 2018 / Accepted: 6 November 2018 / Published online: 23 November 2018

Abstract
In diamond machining of freeform surface on brittle materials, very small machining parameters are necessarily adopted to suppress the brittle fractures, which inevitably leads to low processing efficiency as well as fast tool wear. In the present study, ultra-precision fly cutting is first adopted in processing brittle materials for freeform surfaces to improve machining efficiency and reduce tool wear. In fly cutting, a large swing radius (over 40 mm) is configured between the diamond tool tip and the rotation axis of the spindle, so the workpiece material is intermittently removed by the periodical cut-in and cut-out movement of the diamond tool. The theoretical results show that this unique process generates a very small chip thickness (80 nm) even under large feed rates (9 μm/r) and cutting depths (70 μm), which accordingly improves the machining efficiency without generating brittle fractures. The experimental results show that only 200 min is needed in fly cutting of an F-theta lens with height variation over 50 μm on single-crystal silicon, while over doubled time is needed for conventional slow tool servo. The generated surface is very smooth and uniform with a roughness of only 6 nm Sa. Besides, only micro-ruggedness of diamond tool is formed in fly cutting without the premature appearance of the micro-chips, which enhances tool life and reduces the re-sharpening cost of diamond tools in processing brittle materials.

Keywords Brittle materials · Freeform surfaces · Tool wear patterns · Ultra-precision fly cutting

1 Introduction

The manufacturing of freeform surfaces on brittle materials has attracted widespread attention in an extensive range of applications, such as photoelectronic products, semiconductors, and advanced optics [1, 2]. However, the inherent hard-and-brittle nature of brittle materials, such as silicon, germanium, and silicon carbide, imposes great challenges in obtaining freeform surfaces with ultra-smooth roughness and high form accuracy [2, 3]. For example, the ductile machining depth of silicon generally ranges from 90 nm to less than 200 nm [4], so severe brittle fractures and micro-cracks can propagate into the finished surfaces when adopting a large cutting depth. The necessarily adopted small feed rates and depths of cut inevitably lead to a long processing time and severe tool wear, which highly increase the cost of the products. Even though both traditional and non-traditional machining methods have been proposed for processing brittle materials, it is still a difficult task to improve the machining efficiency and enhance tool life in the machining of freeform surfaces on brittle materials.

A few non-mechanical technologies based on the etching process, such as laser-assisted etching and lithography, have been used for the fabrication of silicon micro-structures [5, 6]. For example, a type of dry etching method based on the femtosecond laser modification was proposed by Liu et al. [7], to fabricate three-dimensional micro-structures on silicon wafers, such as micro gears. However, the etching effects and speed always possess directionality and difficult to be precisely controlled, which highly limit the etching technology in fabricating arbitrarily shaped freeform surfaces or structures on brittle materials. Femtosecond laser polymerization is a promising method to form freeform surface in a flexible way, but this method highly restricts to low efficiency and photocurable polymer materials. More importantly, the surface roughness and form accuracy acquired by these non-mechanical technologies are generally high in terms of optical application. Due to the low

✉ Suet To
sandy.to@polyu.edu.hk

[1] State Key Laboratory in Ultra-precision Machining Technology, Department of Industrial and Systems Engineering, The Hong Kong Polytechnic University, Kowloon, Hong Kong

machining efficiency and the insufficient machining accuracy, it is difficult for these non-mechanical methods to generate arbitrarily shaped freeform surfaces with nanometric surface roughness and sub-micrometric form accuracy [8]. Further, the geometries and shapes possible to be fabricated by etching methods are very limited.

Compared with non-mechanical methods and the abrasive machining technologies, diamond cutting technologies are more flexible in the processing of brittle materials for freeform surfaces, due to their capability of achieving sub-micrometric form accuracy [9–11]. The diamond cutting technologies applied for freeform surfaces can be roughly divided into diamond milling and fast or slow tool servo (FTS/STS). Mukaida et al. successfully fabricated a few micro-lens arrays of silicon via slow tool servo [9]. They demonstrated that smooth surfaces with a surface roughness of 4 nm can be achieved under a very small feed rate. Alvarez lens of germanium were also successfully fabricated by Brian et al. [12] using diamond milling. However, small feed rates and depths of cut are necessarily adopted in diamond cutting of brittle materials to ensure the ductile removal of brittle materials, which greatly reduce the machining efficiency and lead to fast tool wear, accordingly greatly increasing the processing cost [13, 14]. The cost can be much higher in the generation of freeform surfaces, due to the irregular surface structures and the ever-changing azimuthal height variation. However, the literature on improving machining efficiency and reducing tool wear in diamond machining freeform surfaces on brittle materials is very limited.

A variety of technologies were proposed to enhance the machinability of brittle materials in diamond cutting, such as laser-assisted cutting [15], ion implantation modification [4], and vibration-assisted machining [16]. Laser-assisted cutting utilizes a high-power laser to locally elevate the temperature of the workpiece surface prior to material removal with a diamond tool. The elevated temperature decreases the fracture strength of brittle materials and promotes the material deformation from brittle to ductile, thereby reducing the cutting force and enhancing tool life. However, the unavoidable thermal deformation induced by the high-power laser lowers the form accuracy of the generated optic components. Ion implantation modification is beneficial in reducing tool wear and increasing the critical depth of cut. However, the modified layer by ion implantation is generally very thin, and the expansive facilities and laborious process further increases the processing cost of brittle materials. Vibration-assisted diamond machining, including non-resonant and resonant models, facilitates the ductile removal of brittle materials by an intermittent machining process. The diamond tool or workpiece under forced vibration inevitably leads to the regular undulation superimposed on the finished surface. In order to decrease the undulation amplitude, a low normal cutting speed is required in practical applications, thus greatly reducing the machining efficiency. Moreover, much of the previous research on the enhancement of the machinability of brittle materials was performed on flat, spherical, or aspherical shapes, whereas research on the pursuit that how to improve machining efficiency and reduce tool wear in processing brittle materials for optical freeform surfaces featuring ultra-smooth surface quality as well as ultra-high form accuracy is very limited.

The performance of the optical components is highly influenced by its surface quality and form accuracy [17]. The investigation on the proper surface assessment method is also very important in the fabrication of optical freeform surfaces. Generally, researchers and engineers apply average profile surface roughness (Ra) to evaluate the finished surface quality, which belongs to one-dimensional roughness parameter. Nevertheless, this kind of surface description can not exactly reflect the quality of a 3D freeform surface. In comparison, three-dimensional images allow for more accurate surface characteristics due to the description of the whole area of the surface, not only a certain profile [18, 19]. Krolczyk et al. [18] applied parametric and non-parametric method to evaluate the finished surface in turning process, to more accurately access the real finished surface quality. They also proved that the application of power spectral density in surface assessment is possible to characterize the surface acquired from turning process [20]. It is known that the changing cutting direction in diamond turning of single-crystal brittle materials will lead to radial-spoke marks on the finished surface, which is difficult to be assessed by Ra. Up to date, many surface assessment methods have been proposed. For optical freeform surface, it is important to apply a 3D surface assessment method and surface topography image to assess the finished surface in diamond machining of brittle materials.

The hard-and-brittle nature of brittle materials can result in severe tool wear in diamond machining process, which not only deteriorates the surface quality but also increases the cost of optical components. In observing diamond tool wear, Keen et al. [21] proposed that fracture of the cutting edge and micro-grooving are the critical damage phenomena. Durazo-Cardenas et al. [22] studied the 3D characteristics of the worn tool in diamond machining of silicon, and they found that the diamond tool with one particular has prolonged tool life. Compared with copper and aluminum, most brittle materials are more likely to chemically react with diamond tools and lead to severe tool wear. Up to date, to prolong the tool life in diamond machining of freeform surface on brittle materials is still a difficult task. The investigation on the reduction of the fracture impacts of brittle materials on diamond tools is important to prolong tool wear and reduce the cost.

In this study, ultra-precision fly cutting technology was first introduced into the machining of brittle materials for freeform surfaces in ductile mode, to reduce the processing time and enhance tool life. The chip formation process of fly cutting on brittle materials is theoretically discussed to analyze its ductile machining mechanism. The unique chip formation process of

fly cutting can generate extremely small chip thickness even under large feed rates and cutting depths, thereby improving the machining efficiency of brittle materials without destroying the finished surface quality. Besides, through reducing the impact of brittle fractures in the cutting region, the premature micro-chips generated on the diamond tool edge can be effectively avoid. Experimental demonstration was also conducted by fabricating F-theta lens on single-crystal silicon, which is a widely applied brittle material, and its machining efficiency, surface quality, and tool wear patterns were compared with that of slow tool servo and diamond turning.

2 Experiment setup

A freeform milling system with five axes is applied in this study to conduct the ultra-precision fly cutting experiments, as shown in Fig. 1. The workpiece material is single-crystal silicon, which is a typical brittle material. The silicon wafer was previously polished to form a perfect plane. The silicon wafer glued on a fixture was fixed on the *b*-axis, and a diamond tool was mounted on the high-speed spindle. Though carefully tuning the angle of b-axis, the planer surface of the workpiece can be parallel to the *x*-axis. Desired freeform surfaces can be produced by conducting the periodic feed movement in *x* direction and raster movement in *y* direction of the rotational spindle.

Two diamond tools with the same edge radius of 0.5 mm are applied in the experiments of diamond turning and fly cutting, respectively, in order to separately observe their tool wear patterns. The rake angle of the diamond tool is − 25°, while the clearance angle is 10°. The machining parameters of diamond turning and fly cutting in the tool wear experiments are shown in Table 1.

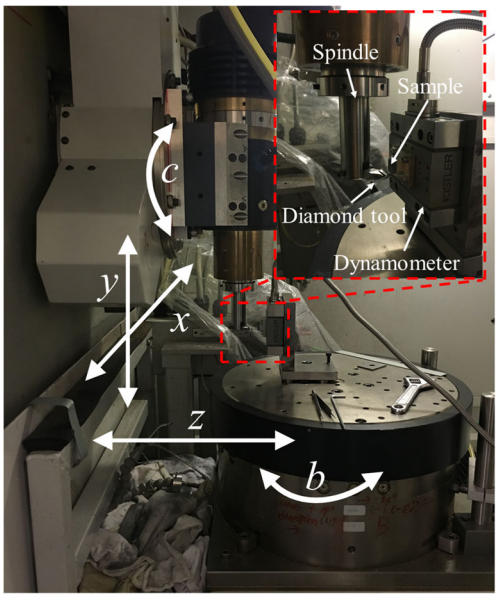

Fig. 1 Hardware configuration of ultra-precision fly cutting

An F-theta lens array is fabricated in this study to validate the proposed method. The mathematical expression of the F-theta surface is $z = a \cdot y^2 + b \cdot x^2 + c \cdot x^4$, with *a*, *b*, and *c* equaling to − 0.0052, − 0.002, and 1.087×10^{-5}, respectively. The machining conditions in fly cutting of F-theta lens array are detailed in Table 2.

After cutting, the surface was cleaned with alcohol to remove the attached chips. The Optical Surface Profiler (Zygo@ Nexview) and Olympus BX60 optical microscope were then employed to capture the topographies of the machined freeform surface with proper magnifications. To map a large area beyond the measurement range, a small group of images were stitched together by using the software system Mx of the Optical Surface Profiler. From the analysis modular of the software, the surface roughness Sa can be directly obtained. As the fabricated F-theta lens is not a plane surface, the primary shape of the selected region is removed by automatic arithmetic of the software system Mx of the Optical Surface Profiler Zygo. Then, the roughness parameter Sa is calculated by the software without other filtering operations. An area surface roughness Sa is adopted to evaluate the surface quality. Sa can be calculated by $\mathrm{Sa} = \left(\frac{1}{\mathrm{MN}}\right) \sum_{i=1}^{N} \sum_{j=1}^{M} |Z_{ij}|$, where *M* and *N* are the sampling number in feed and normal direction respectively and *Zij* is the height of sampling point. A scanning electron microscope was used to observe the tool wear patterns. A Park's XE-70: atomic force microscope (AFM) measurement system was adopted to observe the micro-topography of the generated surface by fly cutting.

3 Chip formation process of fly cutting

Figure 2 schematically illustrates the machining process of fly cutting for optical freeform surfaces. The diamond tool is fixed on the high-speed spindle with a specific swing radius (S_w) that is defined as the maximum distance between the tool tip and the rotational central line of the

Table 1 Machining parameters in the tool wear experiment

Cutting parameters	Diamond turning	Fly cutting
Feed rate (μm/r)	2	7
Depth of cut (μm)	5	10
Spindle rotation rate (rpm)	200	10,000
Swing radius (mm)	None	44.25
Cutting direction	None	<100>

Table 2 Cutting conditions in fly cutting of F-theta lens

Cutting parameters	Fly cutting
Feed rate (μm/r)	7
raster distance (μm)	10
Depth of cut (μm)	5–60
Spindle rotation rate (rpm)	15,000
Swing radius (mm)	44.25
Cutting direction	<100>
Cutting atmosphere	Dry

spindle. During the machining process, the rotating spindle horizontally feeds in the x direction, and the diamond tool intermittently cuts into and out of the workpiece surface. In the meantime, the workpiece performs the transitional servo motions in z direction, just like slow tool servo, to deterministically generate the desired primary surface. After finishing one profile of cutting, a step motion along the raster direction (y direction) is carried out on the diamond tool, so the whole workpiece can be covered by material removal. Through periodic movement of the diamond tool in feed and raster directions, the whole workpiece will be shaped into the desired freeform surfaces. Due to this unique cutting process of fly cutting, its ductile machining mechanism is different from that of milling, grinding, and FTS/STS.

It is known that brittle fractures generate and propagate on the condition that the instantaneous chip thickness exceeds the critical depth of cut (DoC) of silicon the processed brittle material cutting [23, 24]. The chips of fly cutting are intermittently formed by three specific processes, namely, the current rotary cutting, previous rotary

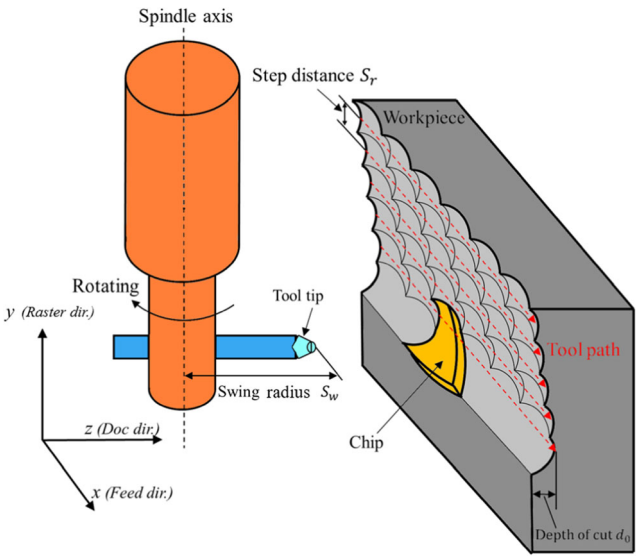

Fig. 2 Schematic illustration of machining principle in fly cutting of micro-grooves

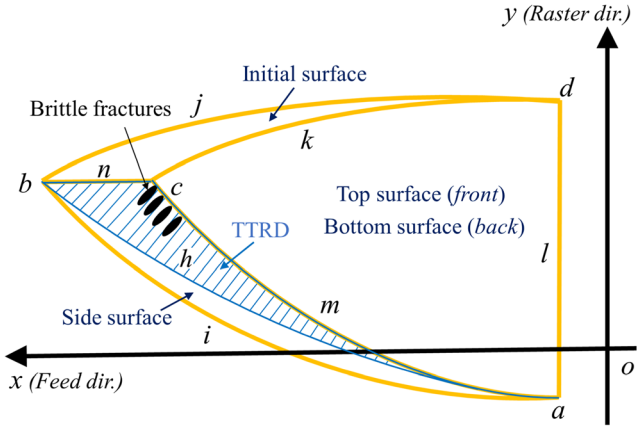

Fig. 3 Schematic illustration of the chip morphology for fly cutting and TTRD

cutting, and previous raster cutting, as illustrated in Fig. 2. As shown in Fig. 3, based on the 3D chip morphology of fly cutting, it is learned that even though the chip thickness changes in both the feed and raster directions, the maximum thickness in the raster direction (TTRD), as marked by the blue lines in Fig. 3, plays a crucial role on the first occurrence of brittle fractures. Therefore, in order to the learn the ductile machining mechanism for fly cutting, the TTRD values at different rotation angles, denoted as h_θ, need to be calculated.

For any chips generated by fly cutting, the h_θ values are equal to the linear distance between the bottom surface of the chip and the curve m and n. As shown in Fig. 4, a system of rectangular coordinates (o-xyz) is defined at the crossing point of the spindle rotational line and the diamond tool holder, with the x axis coincident with the feed direction. As the chip formation duration is extremely short in fly cutting, it is assumed that the spindle is stationary in the chip formation duration when calculating TTRD values. According to the geometric

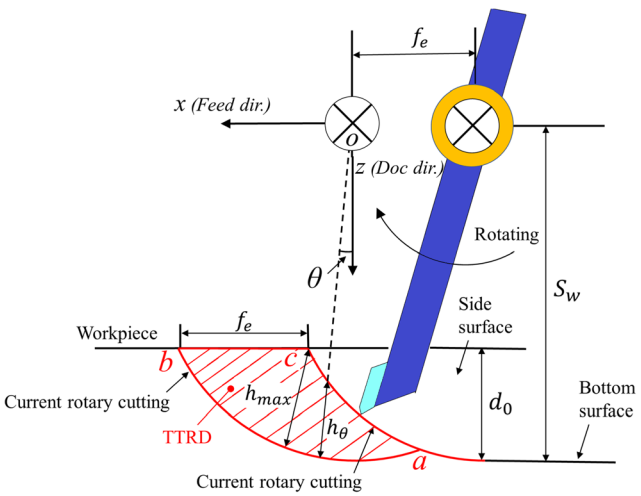

Fig. 4 Schematic of fly cutting viewed along the y direction

relation, the curve m, which is the boundary line between the side and top surface, is expressed as

$$x = \sqrt{s_r(2y+s_r)-2(s_w-R)\left(\sqrt{R^2-(y+s_r)^2}-\sqrt{R^2-y^2}\right)} \quad (1)$$

where s_r denotes the step distance, R represents the edge radius of the diamond tool, and s_w denotes the swing radius. For the boundary line between the initial surface and the side surface (curve n), its equation is given as

$$y = \sqrt{d_0(2R-d_0)}-s_r \quad (2)$$

where d_0 is the depth of cut. Similarly, for boundary line between the bottom and side surface (curve i), its equation is expressed as

$$x = f_e + \sqrt{s_r(2y+s_r)-2(s_w-R)\left(\sqrt{R^2-(y+s_r)^2}-\sqrt{R^2-y^2}\right)} \quad (3)$$

where f_e is the feed rate.

The coordinates of the boundary points can be obtained through calculating the coordinates of the crossing points of their corresponding curves. The crossing point of curves m and i is point a, whose coordinates (x_a, y_a) can be found from Eqs. (1) and (3) as

$$\begin{cases} x_a = f_e/2 \\ y_a = root\ of\left(\sqrt{s_r(2y+s_r)-2(s_w-R)\left(\sqrt{R^2-(y+s_r)^2}-\sqrt{R^2-y^2}\right)}-f_e/2\right) \end{cases} \quad (4)$$

As the mathematical expression for y_a is difficult to express, its value is calculated by solving the above equation.

In the same way, the crossing point of curves n and i is point b, whose coordinates (x_b, y_b) is obtained from Eqs. (2) and (3) as

$$\begin{cases} x_a = f_e/2 + \sqrt{\left(\sqrt{R^2-d_0(2R-d_0)+2s_r\sqrt{d_0(2R-d_0)}-s_r^2}-R+s_w\right)^2-(s_w-d_0)^2} \\ y_a = \sqrt{d_0(2R-d_0)}-s_r \end{cases} \quad (5)$$

As the crossing point of curves n and m is point c, whose coordinates (x_c, y_c) can be obtained from Eqs. (1) and (2) as

$$\begin{cases} x_c = \sqrt{\left(\sqrt{R^2-d_0(2R-d_0)+2s_r\sqrt{d_0(2R-d_0)}-s_r^2}-R+s_w\right)^2-(s_w-d_0)^2} \\ y_c = \sqrt{d_0(2R-d_0)}-s_r \end{cases} \quad (6)$$

Based on Eqs. (5) and (6), the points (x_0, y_0, z_0) on curve n can be given as

$$\begin{cases} x_c \le x_0 \le x_b \\ y_0 = \sqrt{d_0(2R-d_0)}-s_r \\ z_0 = s_w-d_0 \end{cases} \quad (7)$$

In the same way, the points (x_0, y_0, z_0) on curve m can be calculated by

$$\begin{cases} x_0 = \sqrt{s_r(2y_0+s_r)-2(s_w-R)\left(\sqrt{R^2-(y_0+s_r)^2}-\sqrt{R^2-y_0^2}\right)} \\ y_a \le y_0 \le y_c \\ z_0 = s_w-R+\sqrt{R^2-(y_0+s_r)^2} \end{cases} \quad (8)$$

Curve h is acquired by the projection of the curve m and n on the bottom surface, so the coordinates of curve h (x_1, y_1, z_1) can be obtained by the calculation of the crossing points between the bottom surface and the linear line that passes through the $(f_e, 0, 0)$ and (x_0, y_0, z_0). The equation of the straight line can be derived as

$$\frac{x-f_e}{x_0-f_e} = \frac{y}{y_0} = \frac{z}{z_0} \quad (9)$$

The expression of the bottom surface is given as

$$\left(\sqrt{(x-f_e)^2+z^2}-s_w+R\right)^2+y^2 = R^2 \quad (10)$$

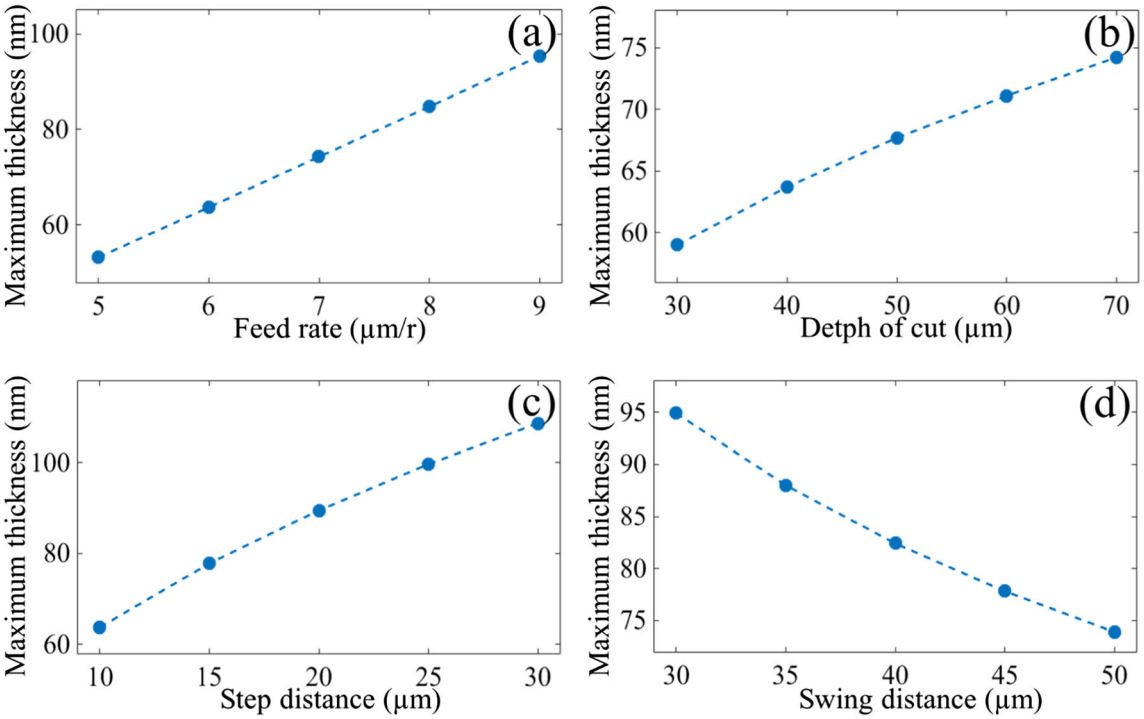

Fig. 5 Variation of TTSD values with **a** depths of cut and **b** feed rates

According to Eqs. (9) and (10), the coordinate values (x_1, y_1, z_1) of curve h can be calculated as follows:

$$\begin{bmatrix} x_1 \\ y_1 \\ z_1 \end{bmatrix} = K \begin{bmatrix} x_0 - f_e \\ y_0 \\ z_0 \end{bmatrix} \tag{11}$$

where

$$K = \frac{(s_w - R)\sqrt{(x_0 - f_e)^2 + z_0^2} + \sqrt{R^2(x_0 - f_e)^2 + R^2 z_0^2 - y_0^2 s_w(s_w - 2R)}}{(x_0 - f_e)^2 + y_0^2 + z_0^2} \tag{12}$$

TTRD values at different rotation angle, h_θ can be acquired through the calculation of the length between the point (x_0, y_0, z_0) and the point (x_1, y_1, z_1), which yields as

$$h_\theta = \sqrt{(x_1 - x_0)^2 + (y_1 - y_0)^2 + (z_1 - z_0)^2} \tag{13}$$

According to Eqs. (12) and (13), it is seen that TTRD is not only determined by the feed rates and cutting depth, but also is inversely proportional to the length of the swing radius. The maximum chip thickness can be acquired by the calculation of the maximum value of h_θ. This unique mathematical relation indicates that small chip thickness is able to be generated using fly cutting even under large feed rates and cutting depths. In contrast, the chip thickness of milling and turning is highly

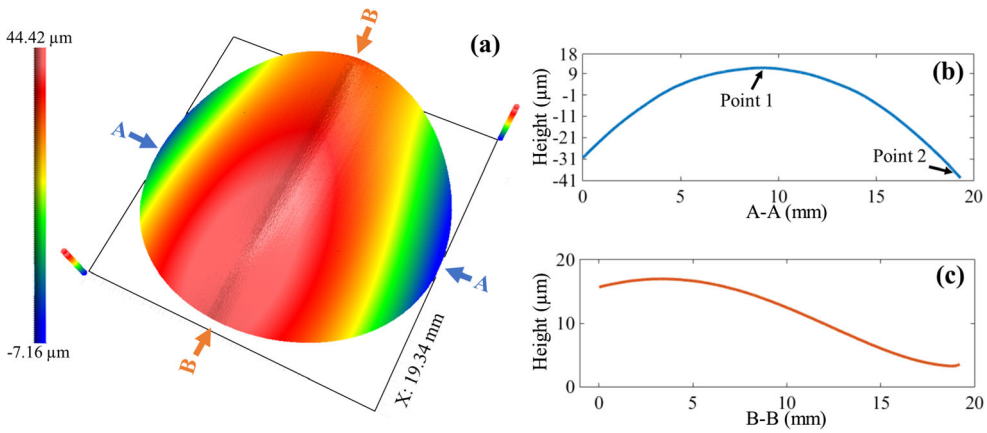

Fig. 6. **a** 3D topography of the generated F-theta surface. **b**, **c** 2D surface profile in the A-A direction and B-B direction

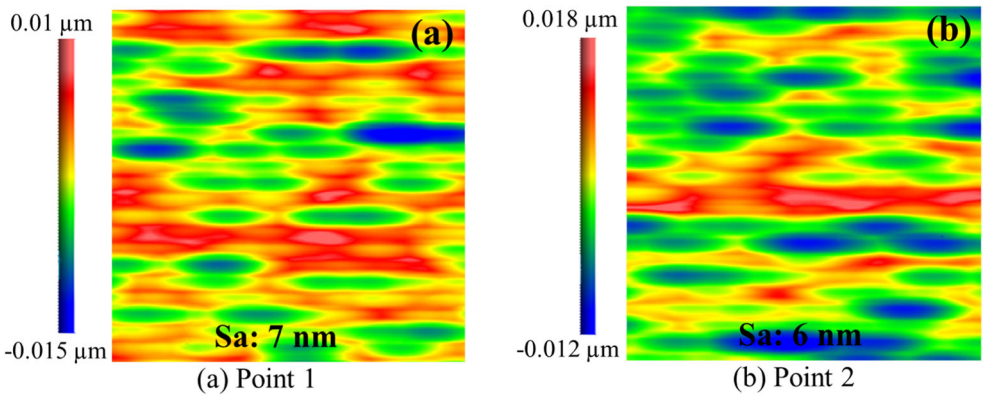

Fig. 7 Micro-surface topographies of **a** point 1 and **b** point 2

influenced by the machining parameters and the tool edge radius, so the employment of very small machining parameters seem to be the only method to reduce the chip thickness [9, 25].

4 Results and discussion

4.1 High efficiency

In the diamond machining of brittle materials, how to prevent the occurrence of brittle fractures under large feed rates and cutting depths is crucial to the improvement of the efficiency. It is known that when the chip thickness is beyond the critical DoC of the fabricated brittle materials, severe brittle fractures will generate in the cutting region [4]. Thus, analyzing the change of the chip thickness under different machining parameters should be conducted before analyzing the machining efficiency for processing brittle materials. According to the chip formation process discussed above, TTRD values actually represent the chip thickness of fly cutting, whose maximum value represents the maximum chip thickness. The brittle material is removed in ductile model when the maximum chip thickness is lower than the critical DoC of silicon. As the critical depth of cut is generally calculated based on the empirical formula [26], the result is not quite accurate. To acquire the accurate critical DoC of silicon, experiment method is applied by sculpturing silicon for a taper groove with increasing cutting depth in this study. The value of the critical DoC is acquired by observing the depth of the brittle-ductile transition boundary. The critical DoC of the silicon wafer is at 148 nm, which is similar to that of previous studies [4].

As shown in Fig. 5, an increasing trend of the maximum chip thickness is acquired with increasing feed rate, cutting depth, and raster distance, while the maximum chip thickness decreases with increasing length of the swing radius. It is interesting to note from the simulation results that the chip thickness of fly cutting is far less than the adopted feed rates and depths of cut. For instance, the maximum chip thickness of fly cutting under a cutting depth of 70 μm and feed rate of 9 μm/r is only estimated at 80 nm. From the chip formation process of fly cutting, it is learned that the extremely small chip thickness of fly cutting majorly results from the unique cutting process of fly cutting, in which the diamond tool rotates with a large swing radius in the normal plane of the workpiece surface. This unique cutting trajectory leads to the inverse proportional relation between the chip thickness and the swing radius, as expressed in Eqs. (12) and (13). Based on this mathematical relation, it is found that through configuring a large swing radius, the chip thickness will be reduced to an extremely small value even under large feed rates and depths of cut, thereby ensuring the ductile processing of brittle materials for freeform surfaces with high efficiency.

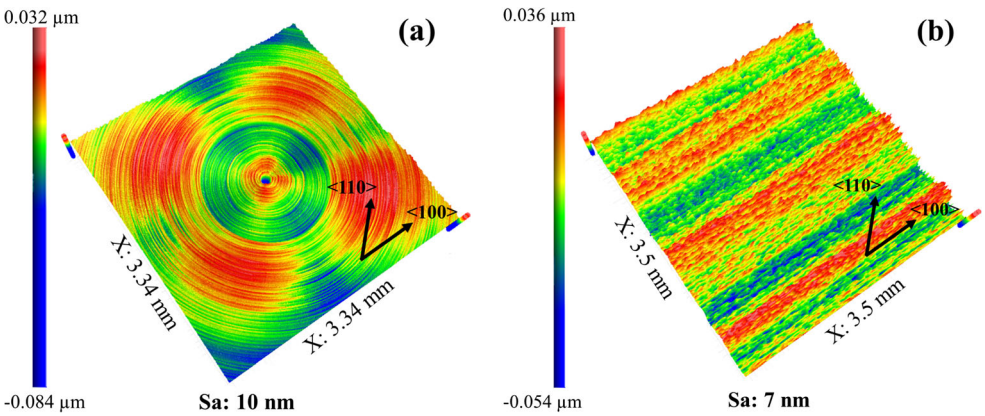

Fig. 8 Surface topographies of silicon generated via **a** turning and **b** fly cutting

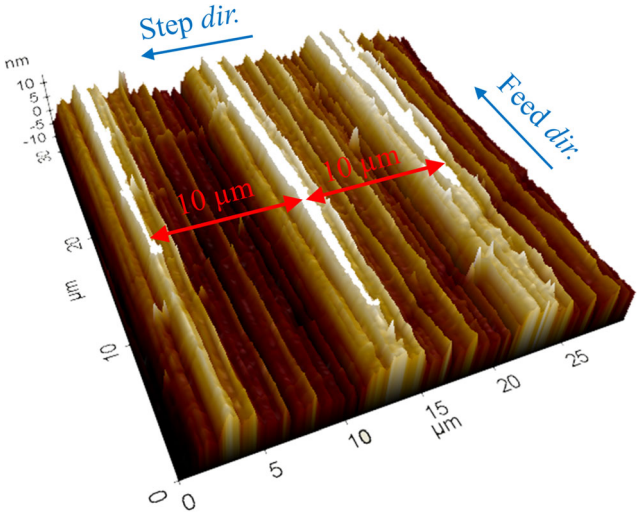

Fig. 9 Micro-topography of the surface generated by fly cutting

To validate the superiority of the proposed method in the ductile processing of brittle materials for freeform surfaces with high efficiency, an F-theta freeform surface is directly fabricated by fly cutting on single-crystal silicon. Figure 6a shows the 3D surface topography of the F-theta lens, and Fig. 6b, c shows the cross profiles along the A-A and B-B directions. Smooth surface quality without brittle fractures was observed from both the 3D surface topography and the cross profiles, indicating the ductile material removal process. Furthermore, as shown in Fig. 6b, the height variation of the generated surface is over 50 μm at point 1 and point 2, which means the value difference between their cutting depths is also over 50 μm. Nevertheless, in the micro-topographies of point 1 and point 2 shown in Fig. 7a, b, no brittle fractures were observed at the two points, and their surface roughness is similar, measured at 7 and 6 nm, respectively. This validates the advantage of fly cutting in the generation of freeform surfaces featuring large height variation without brittle fractures. This is majorly attributed to the rotational cutting trajectory with a large swing radius in fly cutting, so even though the cutting depth greatly changes in the machining of freeform surfaces, the variation of chip thickness is less than 30 nm, as illustrated in Fig. 5b.

The processing time of the F-theta lens is about 200 min by fly cutting under the machining parameters shown in Table 2. Nevertheless, if applying slow tool servo (STS) or diamond milling technologies to fabricate the same F-theta lens on single-crystal silicon, the machining time is estimated over 450 min, based on the machining parameters provided in the literature [9, 27]. The main reason for the low machining efficiency of STS and diamond in the processing of brittle materials is the necessarily adopted low feed rates and cutting depths to suppress the brittle fractures. Especially, when fabricating freeform surfaces with tens of micrometers height variation, repeated cutting processes with each cycle operated under a small depth of cut have to be employed until reaching the desired depth. Further, the limited dynamic response ability of ultra-precision machine tools restricts the maximum spindle speed of STS when processing brittle materials, which also highly prolongs the machining time [9, 28].

4.2 Surface quality

It is known that the ductile machining models for FTS/STS is similar to that of turning [25], where the cutting direction is ever-changing in relation to the crystal orientations of single-crystal brittle materials. This ever-changing cutting direction can result in a highly non-uniform surface quality of some single-crystal brittle materials due to their anisotropic properties. As shown in Fig. 8a, the finished surface generated by diamond turning is highly non-uniform and characterized as radial-spoke marks, which can highly deteriorate the imaging quality of infrared optics [9]. Particularly, this non-uniform surface quality becomes more obvious when machining with large feed rates, due to the different critical DoC in different crystal orientations of single-crystal brittle materials, which further reduce the efficiency of FTS/STS in generating freeform surfaces on single-crystal IR materials.

In contrast, the cutting direction of fly cutting is unchanged, so uniform surface quality with low surface roughness is able to be generated, as shown in Fig. 8b. Moreover, through

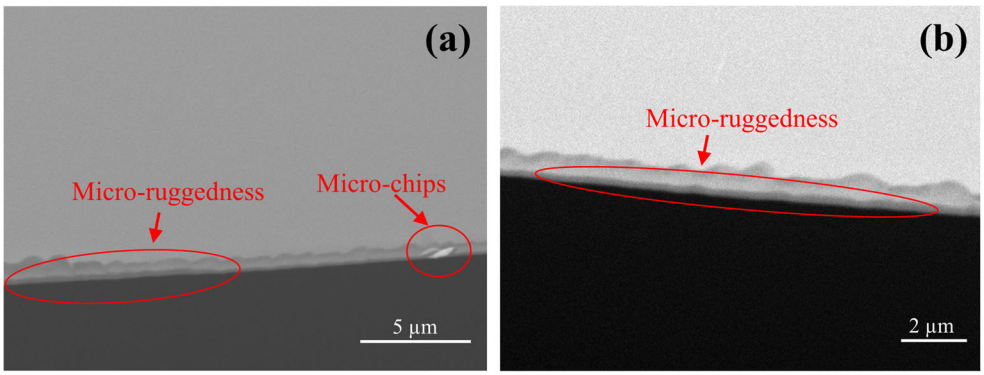

Fig. 10 Tool wear patterns observed by SEM in **a** diamond turning and **b** fly cutting

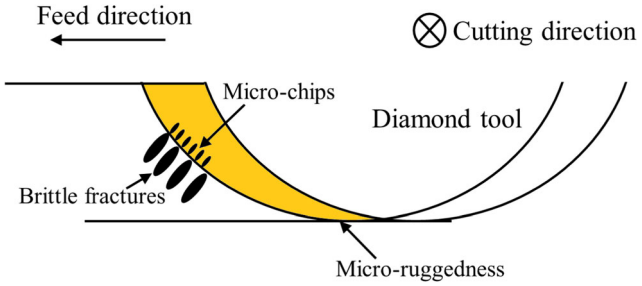

Fig. 11 Schematic illustration of the tool wear patterns of diamond turning

choosing the crystal orientation with larger critical DoC as the feed direction, slightly higher feed rates can be adopted without influencing the acquired surface quality. Therefore, fly cutting can generate freeform optics with a uniform surface quality even under large feed rates and cutting depths.

To further validate the feasibility of fly cutting in processing brittle materials without surface damages, the micro-topography of the generated surface is observed by AFM, as shown in Fig. 9. The micro-topography is characterized by a set of parallel tool marks along feed direction, which is caused by the unique cutting strategy of fly cutting. Periodic peaks along step direction with an equal distance of 10 μm are in accordance with the adopted raster distance as shown in Table 2. This indicates that the obtained surface micro-topography is highly determined by the raster distance of fly cutting. It is worth to note that apart from the parallel tool marks, no other types of damages or brittle fractures can be observed on the micro-topography, which validates the feasibility of fly cutting in the processing of brittle materials with high surface quality.

4.3 Tool wear

Figure 10a, b compares the different tool wear patterns acquired from turning and fly cutting of single-crystal silicon. To make a comparison, the cutting distance of the two methods is the same at 200 m. As shown in Fig. 10a, two kinds of tool wear patterns are identified in diamond turning: one is the micro-ruggedness distributed at the tool apex (wear width ~300 nm); the other refers to the micro-chips (wear width ~1.2 μm) generated on the cutting edge contacting the uncut surface. As in the ductile machining mechanism of diamond turning illustrated in Fig. 11, the undeformed chip thickness near the tool apex is very small; thus, the workpiece material in this region is removed in ductile model, and the severe abrasion between the tool edge and workpiece material leads to the micro-ruggedness. On the other hand, with the increase of the undeformed chip thickness along the tool edge, brittle fractures easily occur at a lager chip thickness. This brittle material removal behavior inevitably results in an intermittent impact to the tool edge, which then causes the generation of micro-chips on the tool edge in this region [9, 29].

In contrast, only micro-ruggedness with a smaller wear width ~210 nm was observed in fly cutting, as shown in Fig. 10b. According to the chip formation process of fly cutting, the chip thickness remains smaller than the critical DoC of silicon, indicating that the workpiece material is removed in a ductile model without brittle fractures. As a result, the smaller wear width of fly cutting (~210 nm) compared with that of diamond turning (~300 nm) is probably due to the better lubrication and better chip removal process of the intermittent cutting process of fly cutting. It is known that compared with micro-ruggedness, the re-sharpening behavior of micro-chips generally needs an extended grinding time as well as a large volume of diamond being removed, which finally highly increase the cost of the corresponding products. As a result, the totally ductile material removal behavior of fly cutting can reduce the process cost of brittle materials through avoiding the generation of premature micro-chips on the diamond tool edge.

To further study the tool wear state in fly cutting of brittle materials, a longer cutting distance of 700 m was adopted before observing the tool wear patterns. Figure 12a, b shows the rake face and flank face of the diamond tool in fly cutting of single-crystal silicon after a distance of 700 m. For the rake

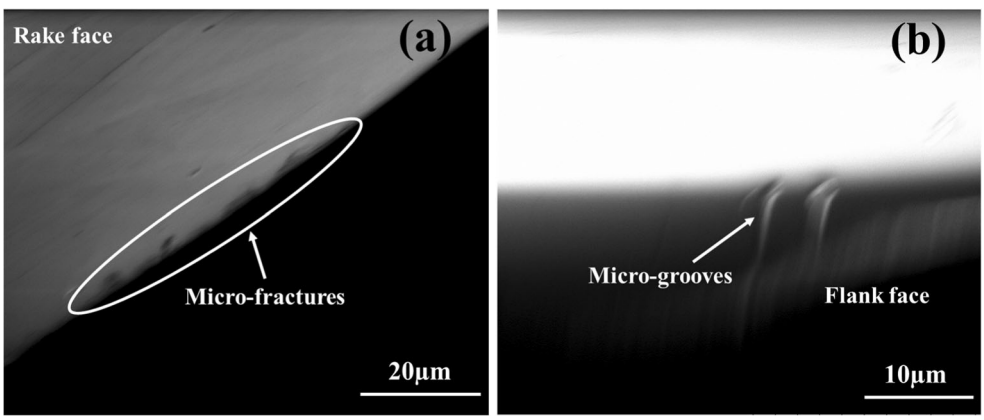

Fig. 12 SEM images of tool edge after raster milling single-crystal silicon. **a** Rake face. **b** Flank face

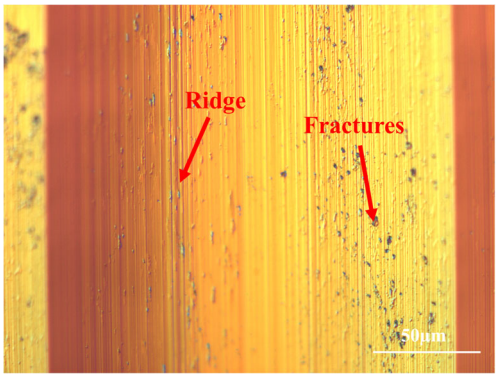

Fig. 13 Optical microscopy of the bottom surface after raster milling for 700 m

face, a few micro-fractures were observed at the tool apex, which is caused by the combined effect of the abrasive effect under the high hydrostatic pressure in the cutting area. It is observed that the micro-fractures of diamond tool appear in fly cutting after cutting a much longer distance compared with that of turning, which validates the longer tool life of fly cutting. As most of the literature reported, high pressure phase transformation (HPPT) is regarded as primary mechanism of the plasticity of brittle materials [30]. To achieve the ductile model removal of single-crystal silicon, the hydrostatic pressure in the cutting area has to reach about 12 GPa [31, 32]. Thus, it is learned that the abrasive effect between the diamond tool and silicon under such high pressure combined with the intermittent cutting force of fly cutting induce micro-fractures on the tool rake face.

On the other hand, the high hydrostatic pressure and the accumulated cutting temperature in the cutting region can provide the necessary condition for the tribo-chemical reaction between the diamond and silicon and generates silicon carbide (SiC) and diamond-like carbon structures on the tool surface [33]. It is known that the hardness of SiC is comparable to that of diamond crystal at nanometric scale [34]. As a result, the severe plowing and scratching of SiC and diamond-like carbon structures with diamond tools induces the micro-grooves left on the flank face and parallel to the cutting direction, as shown in Fig. 12b. Therefore, it learns that micro-fractures and micro-grooves are the two patterns of the tool wear in fly cutting after cutting a long distance. During the ultra-precision machining operation, the micro-fractures and the micro-grooves on the diamond tool can be directly imprinted on the finish surface of single-crystal silicon. Besides, the decrease of cutting edge radii caused by the micro-grooves tends to change the machining model from ductile to brittle. The destroyed surface of single-crystal silicon machined by a worn diamond tool is shown in Fig. 13, where a group of "ridges" and fractured surface can be clearly observed on the bottom surface.

5 Conclusions

The hard-and-brittle nature of brittle materials inevitably leads to very long processing time and fast tool wear in the fabrication of freeform surfaces using ultra-precision machining methods. In the present study, ultra-precision fly cutting technology is first introduced in the processing of brittle materials for freeform surfaces to improve the machining efficiency and reduce tool wear. The chip formation process in fly cutting of brittle materials is theoretically simulated for the first time, which well explains why large feed rates and depths of cut can be adopted by fly cutting in the processing of brittle materials without leading to fractured surfaces. Experimental validation is also conducted through fabricating an optical F-theta lens on single-crystal silicon. After comparing the machining efficiency, surface quality, and tool wear patterns with that of conventional slow tool servo turning, specific conclusions can be drawn as follows:

1. Taking advantage of the large swing radius of fly cutting (over 40 mm), very small chip thickness (80 nm) can be generated by fly cutting even under very large feed rates (9 μm/r) and depths of cut (70 μm). This unique characteristic of fly cutting can effectively suppress brittle fractures in the fabrication of freeform surface even under large machining parameters.
2. An F-theta lens with the AHV over 50 μm is successfully produced by fly cutting on single-crystal silicon. Very smooth and uniform surface with a roughness of 6 nm Sa is acquired. The machining time is about 200 min, which is less than half of the time needed in slow tool servo.
3. The unchanged cutting direction of fly cutting is able to prevent the unavoidable radial-spoke marks of single-crystal silicon generated in diamond turning and slow tool servo technologies, thereby improving the surface quality. The micro-topography of the generated freeform surface is also very smooth without damages.
4. After a cutting distance of 200 m, only ~210 nm wide micro-ruggedness was observed in fly cutting, while much wider micro-chips with 1.2 μm width was generated by diamond turning. The smaller wear width well validates the enhanced tool life of fly cutting in processing brittle materials compared with conventional diamond turning.
5. This research provides an efficient method to fabricate freeform surfaces featuring ultra-smooth surface roughness on brittle materials, with improved machining efficiency and reduced tool wear. It is worth to note that the large swing radius of fly cutting limits its application in fabricating concave micro-structures with large curvature.

Funding information This work was supported partially by the Research Committee of The Hong Kong Polytechnic University (Project Code: RUNS).

References

1. Hong Z, Liang R (2017) IR-laser assisted additive freeform optics manufacturing. Sci Rep 7:7145
2. Zhu L, Li Z, Fang F, Huang S, Zhang X (2018) Review on fast tool servo machining of optical freeform surfaces. Int J Adv Manuf Technol 95:2071–2092
3. Liu H, Xie W, Sun Y, Zhu X, Wang M (2018) Investigations on brittle-ductile cutting transition and crack formation in diamond cutting of mono-crystalline silicon. Int J Adv Manuf Technol 95: 317–326
4. Xiao G, To S, Jelenković E (2015) Effects of non-amorphizing hydrogen ion implantation on anisotropy in micro cutting of silicon. J Mater Process Technol 225:439–450
5. Pachaury Y, Tandon P (2017) An overview of electric discharge machining of ceramics and ceramic based composites. J Manuf Process 25:369–390
6. Azarhoushang B, Soltani B, Zahedi A (2017) Laser-assisted grinding of silicon nitride by picosecond laser. Int J Adv Manuf Technol 93:2517–2529
7. Liu X-Q, Yu L, Ma Z-C, Chen Q-D (2017) Silicon three-dimensional structures fabricated by femtosecond laser modification with dry etching. Appl Opt 56:2157–2161
8. Hourmand M, Sarhan AA, Sayuti M (2017) Micro-electrode fabrication processes for micro-EDM drilling and milling: a state-of-the-art review. Int J Adv Manuf Technol 91:1023–1056
9. Mukaida M, Yan J (2017) Ductile machining of single-crystal silicon for microlens arrays by ultraprecision diamond turning using a slow tool servo. Int J Mach Tools Manuf 115:2–14
10. Zhang S, Yu J, To S, Xiong Z (2018) A theoretical and experimental study of spindle imbalance induced forced vibration and its effect on surface generation in diamond turning. Int J Mach Tools Manuf 133:61–71
11. Sun Z, To S, Zhang S, Zhang G (2018) Theoretical and experimental investigation into non-uniformity of surface generation in micro-milling. Int J Mech Sci 140:313–324
12. Dutterer BS, Lineberger JL, Smilie PJ, Hildebrand DS, Harriman TA, Davies MA, Suleski TJ, Lucca DA (2014) Diamond milling of an Alvarez lens in germanium. Precis Eng 38:398–408
13. Bai J, Bai Q, Hu C, He X, Pei X (2018) Research on the ductile-mode machining of monocrystalline silicon using polycrystalline diamond (PCD) tools. Int J Adv Manuf Technol 94:1981–1989
14. Bian R, He N, Ding W, Liu S (2017) A study on the tool wear of PCD micro end mills in ductile milling of ZrO2 ceramics. Int J Adv Manuf Technol 92:2197–2206
15. Przestacki D, Chwalczuk T, Wojciechowski S (2017) The study on minimum uncut chip thickness and cutting forces during laser-assisted turning of WC/NiCr clad layers. Int J Adv Manuf Technol 91:3887–3898
16. X.-F. Song, J.-J. Yang, H.-T. Ren, B. Lin, Y. Nakanishi, L. Yin (2018) Ultrasonic assisted high rotational speed diamond machining of dental glass ceramics, Int J Adv Manuf Technol 1–13
17. Huo D (2013) Micro-cutting: fundamentals and applications. John Wiley & Sons
18. Krolczyk G, Maruda R, Krolczyk J, Nieslony P, Wojciechowski S, Legutko S (2018) Parametric and nonparametric description of the surface topography in the dry and MQCL cutting conditions. Measurement 121:225–239
19. Grabon W, Pawlus P (2018) Improvement of the Rpq parameter calculation. Measurement 129:236–244
20. Krolczyk G, Maruda R, Nieslony P, Wieczorowski M (2016) Surface morphology analysis of duplex stainless steel (DSS) in clean production using the power spectral density. Measurement 94:464–470
21. Keen D (1971) Some observations on the wear of diamond tools used in piston machining. Wear 17:195–208
22. Durazo-Cardenas I, Shore P, Luo X, Jacklin T, Impey S, Cox A (2007) 3D characterisation of tool wear whilst diamond turning silicon. Wear 262:340–349
23. Sun Z, To S, Yu K (2018) One-step generation of hybrid micro-optics with high-frequency diffractive structures on infrared materials by ultra-precision side milling. Opt Express 26:28161–28177
24. Wang H, Riemer O, Rickens K, Brinksmeier E (2016) On the mechanism of asymmetric ductile–brittle transition in microcutting of (111) CaF2 single crystals. Scr Mater 114:21–26
25. Blake PN, Scattergood RO (1990) Ductile-regime machining of germanium and silicon. J Am Ceram Soc 73:949–957
26. Goel S, Luo X, Comley P, Reuben RL, Cox A (2013) Brittle–ductile transition during diamond turning of single crystal silicon carbide. Int J Mach Tools Manuf 65:15–21
27. Arif M, Rahman M, San WY (2012) An experimental investigation into micro ball end-milling of silicon. J Manuf Process 14:52–61
28. Yu D, Wong Y, Hong G (2011) Ultraprecision machining of micro-structured functional surfaces on brittle materials. J Micromech Microeng 21:095011
29. Sun Z, To S, Zhang S (2018) A novel ductile machining model of single-crystal silicon for freeform surfaces with large azimuthal height variation by ultra-precision fly cutting. Int J Mach Tools Manuf 135:1–11
30. Goel S, Luo X, Agrawal A, Reuben RL (2015) Diamond machining of silicon: a review of advances in molecular dynamics simulation. Int J Mach Tools Manuf 88:131–164
31. Skorupa W, Yankov R (1996) Carbon-mediated effects in silicon and in silicon-related materials. Mater Chem Phys 44:101–143
32. Sanz-Navarro C, Kenny S, Smith R (2004) Atomistic simulations of structural transformations of silicon surfaces under nanoindentation. Nanotechnology 15:692–697
33. Zong W, Sun T, Li D, Cheng K, Liang Y (2008) XPS analysis of the groove wearing marks on flank face of diamond tool in nanometric cutting of silicon wafer. Int J Mach Tools Manuf 48:1678–1687
34. Pantea C (2004) Kinetics of diamond-silicon reaction under high pressure-high temperature conditions